Global biogeography of fungal and bacterial biomass carbon in topsoil

Liyuan He [a], Jorge L. Mazza Rodrigues [b], Nadejda A. Soudzilovskaia [c], Milagros Barceló [c], Pål Axel Olsson [d], Changchun Song [e], Leho Tedersoo [f], Fenghui Yuan [a,g], Fengming Yuan [h], David A. Lipson [a], Xiaofeng Xu [a,*]

[a] Biology Department, San Diego State University, San Diego, CA, 92182, USA
[b] Department of Land, Air and Water Resources, University of California Davis, Davis, CA 95616, USA
[c] Environmental Biology Department; Institute of Environmental Sciences, CML, Leiden University; Einsteinweg 2, 2333 CC Leiden, the Netherlands
[d] Biodiversity, Biology Department, Lund University, SE-223 62 Lund, Sweden
[e] Northeast Institute of Geography and Agroecology, Chinese Academy of Sciences, Changchun, 130102, China
[f] Institute of Ecology and Earth Sciences, University of Tartu, 14a Ravila, 50411 Tartu, Estonia
[g] Shenyang Institute of Applied Ecology, Chinese Academy of Sciences, Shenyang, 110016, China
[h] Oak Ridge National Laboratory, Environmental Sciences Division, Oak Ridge, TN, USA

ARTICLE INFO

ABSTRACT

Bacteria and fungi, representing two major soil microorganism groups, play an important role in global nutrient biogeochemistry. Biogeographic patterns of bacterial and fungal biomass are of fundamental importance for mechanistically understanding nutrient cycling. We synthesized 1323 data points of phospholipid fatty acid-derived fungal biomass C (FBC), bacterial biomass C (BBC), and fungi:bacteria (F:B) ratio in topsoil, spanning 11 major biomes. The FBC, BBC, and F:B ratio display clear biogeographic patterns along latitude and environmental gradients including mean annual temperature, mean annual precipitation, net primary productivity, root C density, soil temperature, soil moisture, and edaphic factors. At the biome level, tundra has the highest FBC and BBC densities at 3684 (95% confidence interval: 1678–8084) mg kg^{-1} and 428 (237–774) mg kg^{-1}, respectively; desert has the lowest FBC and BBC densities at 16.92 (14.4–19.89) mg kg^{-1} and 6.83 (6.1–7.65) mg kg^{-1}, respectively. The F:B ratio varies dramatically, ranging from 1.8 (1.6–2.1) in savanna to 8.6 (6.7–11.0) in tundra. An empirical model was developed for the F:B ratio and it is combined with a global dataset of soil microbial biomass C to produce global maps for FBC and BBC in 0–30 cm topsoil. Across the globe, the highest FBC is found in boreal forest and tundra while the highest BBC is in boreal forest and tropical/subtropical forest, the lowest FBC and BBC are in shrub and desert. Global stocks of living microbial biomass C were estimated to be 12.6 (6.6–16.4) Pg C for FBC and 4.3 (0.5–10.3) Pg C for BBC in topsoil. These findings advance our understanding of the global distribution of fungal and bacterial biomass, which facilitates the incorporation of fungi and bacteria into Earth system models. The global maps of bacterial and fungal biomass serve as a benchmark for validating microbial models in simulating the global C cycle under a changing climate.

1. Introduction

Microorganisms play an essential role in soil carbon (C) and nutrient biogeochemistry impacting on various ecosystem processes, including organic matter mineralization, soil formation, and nutrient availability (Högberg et al., 2001;Rillig and Mummey, 2006; Turner et al., 2013; Crowther et al., 2019; Xu et al., 2014). Eventually, the ultimate fate of soil C is driven by microbes (Schimel and Schaeffer, 2012). Although the critical roles of soil microbes in global C and nutrient cycling have been widely recognized (Falkowski et al., 2008; van der Heijden et al., 2008), the research on biogeographic distribution of fungi and bacteria is still in its infancy (Fenchel, 2002; Boer et al., 2005; Rousk and Bååth, 2011; Gougoulias et al., 2014). Furthermore, microbial community structure is an important factor controlling C and nutrient biogeochemistry as bacteria and fungi differ in enzyme production, C use efficiency, and carbon:nitrogen ratio (Caldwell, 2005; Six et al., 2006; Mouginot et al., 2014), and respond differently to multiple global change factors (Rousk and Bååth, 2011; Rousk et al., 2010). Therefore, biogeographic patterns

---

of bacteria and fungi provide pivotal information for understanding microbial contributions to global C and nutrient biogeochemistry.

Geographic distribution of soil microbes is driven by a suite of abiotic and biotic factors (Martiny et al., 2006; Hanson et al., 2012). Previous studies have investigated the factors controlling microbial diversity and functions, including soil organic C (SOC), climate, and vegetation (de Vries et al., 2012). Soil moisture (SM), soil organic matter quality, and soil pH are among the most important factors influencing soil microbial community composition (Fierer and Jackson, 2006; Eskelinen et al., 2009; Brockett et al., 2012; Ding et al., 2015). Although these findings provide valuable information for local to regional environmental drivers and proxies of soil microbial community structure, a holistic and quantitative understanding of soil biogeography of different microbial groups are lacking at the global scale. In particular, the lack of clear quantitative understanding of bacterial and fungal biogeography and their controls hinders the explicit incorporation of microbial mechanisms into climate models (DeLong et al., 2011; Wieder et al., 2013; Xu et al., 2014, 2020).

To fill the knowledge gaps in biogeographic patterns for fungi and bacteria, we compiled a global dataset of 1323 sets of phospholipid fatty acid (PLFA)-derived fungal biomass C (FBC), bacterial biomass C (BBC), and fungi:bacteria (F:B) ratio in topsoil (0–30 cm). FBC and BBC derived from other approaches (primarily microscopic counting, colony forming units, substrate-induced respiration, and glucosamine and muramic acid) were excluded from this study due to large biases in reported values by various approaches. The PLFA was the most widely used and likely the most appropriate approach for estimating FBC and BBC simultaneously (Waring et al., 2013). In this study, we aimed to answer three research questions with the comprehensive dataset of FBC, BBC, and F:B ratio: 1) What are the biogeographic patterns of BBC, FBC, and F:B ratio in topsoil? 2) What are the environmental controls of the biogeographic patterns of fungal and bacterial biomass C? 3) What are the budgets of FBC and BBC at biome and global scales?

2. Materials and Methods

2.1. Data compilation

We used a combination of keywords, "fung*" or "bacteria*", "ratio", and "terrestrial" or "soil", to search peer-reviewed papers in Google Scholar. The papers were selected via the following criteria: 1) either concurrent fungal biomass and bacterial biomass or F:B ratio was clearly reported; 2) the data were extractable from tables (assessing the text) or figures (using Engauge Digitizer Version 10.7); 3) the study sites were not affected by disturbances such as fire, mining, and heavy metal contamination; and 4) the reported data cover 0–30 cm topsoil. Geographical information of the sampling sites was recorded and used to locate the sites on the global map (Fig. 1). We also collected any available data on soil pH, mean annual precipitation (MAP), mean annual temperature (MAT), SOC, total nitrogen (TN) concentration, and soil texture, and then plotted these variables against the extracted data from global datasets to test the consistency (Fig. S1).

We recorded fungal and bacterial biomass C measured using methods such as phospholipid fatty acid (PLFA), direct microscopy (DM), colony forming units (CFU), substrate-induced respiration (SIR), and glucosamine and muramic acid (GMA) from peer-reviewed papers. To examine the potential biases in the measurement of fungal and bacterial biomass, we did a comparison among those methods (Table 1, Table S1). To compare FBC and BBC measured using different methods, we used conversion factors for PLFA Frostegård and Bååth, 1996; Klamer and Bååth, 2004), SIR (Beare et al., 1990), CFU (Aon et al., 2001), DM (Birkhofer et al., 2008), and GMA (Jost et al., 2011) reported in previous studies. Across biomes, FBC, BBC, and the F:B ratio generally followed a similar pattern among different methods. However, large variations were found in measured FBC and BBC among different methods. Specifically, compared with PLFA, SIR, and GMA, CFU reported dominant fungi over bacteria, while DM estimated a higher dominance of bacteria relative to fungi, suggesting that DM may underestimate FBC while CFU may overestimate FBC. Meanwhile, we found overall higher FBC and BBC measured using GMA, which was largely distinct from the measurements using other methods. Using data generated from multiple methods in one analysis might be problematic. Therefore, we used PLFA data for subsequent analyses. This selection was due to two reasons: 1) the PLFA was the most widely used approach, with the PLFA-derived FBC and BBC measurements accounting for 73% of the whole dataset; 2) the PLFA method has been evaluated and proved to be the most appropriate approach for estimating FBC and BBC simultaneously (Waring et al., 2013).
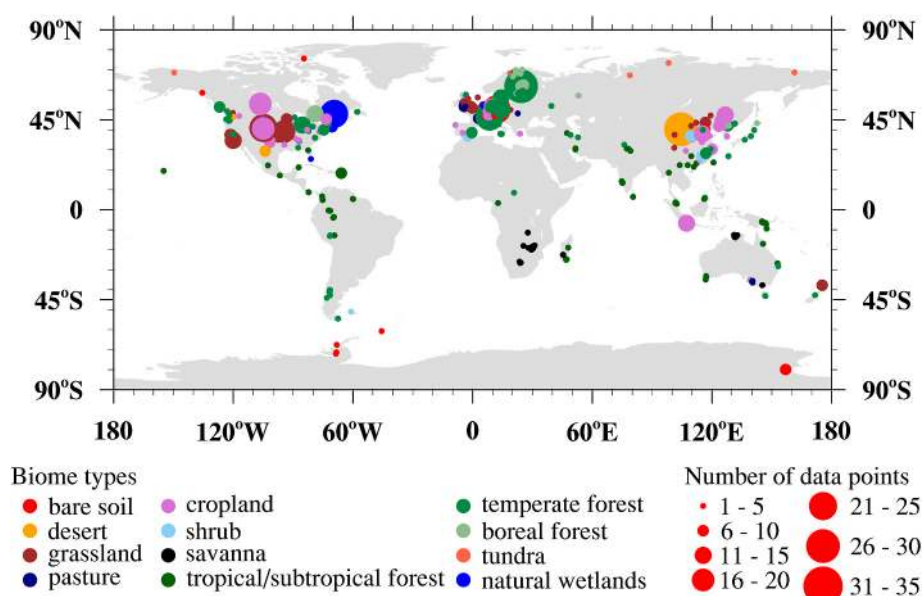

Fig. 1. Global distribution of data points included in this analysis. 1323 data points with geographical coordinates are shown in this map. Circles indicate study sites, with circles in different sizes showing variation in the number of data points and different colors representing different biomes. (For interpretation of the references to color in this figure legend, the reader is referred to the Web version of this article.)

Table 1
Biome-level fungal biomass carbon (FBC), bacterial biomass carbon (BBC) and fungi: bacteria (F:B) ratio.

Biome	FBC (mg kg^{-1} soil)	BBC (mg kg^{-1} soil)	F:B ratio
Unvegetated ground	192.74[de] (54.79–677.99)	24.60[d] (7.68–78.72)	3.90[bc] (2.20–6.91)
Desert	16.92[f] (14.40–19.89)	6.83[e] (6.10–7.65)	3.14[bcd] (2.20–4.49)
Grassland	215.19[de] (168.98–274.03)	62.69[cd] (50.44–77.92)	4.03[b] (3.52–4.62)
Pasture	632.15[bc] (288.99–1382.81)	270.65[a] (129.07–567.53)	2.48[cde] (1.62–3.80)
Cropland	212.69[de] (150.35–300.88)	65.77[cd] (46.30–93.42)	3.28[bcd] (2.89–3.73)
Shrub	218.14[cde] (106.01–448.9)	45.42[cd] (23.48–87.85)	4.82[b] (3.72–6.25)
Savanna	103.36[e] (60.62–176.23)	44.37[cd] (25.94–75.92)	1.82[e] (1.57–2.11)
Tropical/ subtropical forest	451.40[bc] (362.32–562.39)	209.96[ab] (179.03–246.24)	2.22[de] (1.87–2.63)
Temperate forest	258.39[de] (189.16–352.95)	53.05[cd] (38.71–72.70)	4.92[b] (4.39–5.51)
Boreal forest	1234.08[b] (870.72–1749.08)	226.37[ab] (172.79–296.58)	5.03[b] (4.23–5.98)
Tundra	3683.59[a] (1678.49–8083.94)	428.37[a] (236.98–774.31)	8.60[a] (6.71–11.01)
Natural wetlands	329.81[cde] (194.80–558.4)	92.58[bc] (50.99–168.10)	4.13[b] (3.50–4.86)

[a]Values are presented as means with a 95% confidence boundary in parentheses for fungal, bacterial biomass and F:B ratio. Different superscript letters in one column mean significant difference at the significance level of $P = 0.05$, while the same letters indicate no significant difference.

The final database included the fungal and bacterial biomass data measured using PLFA from publications spanning from the late 1960s to 2018. Collectively, 1323 data points in 11 biomes (i.e., boreal forest, temperate forest, tropical/subtropical forest, grassland, shrub, savanna, tundra, desert, natural wetlands, cropland, and pasture) across the globe were included in the database (Fig. 1). Forest, grassland, and cropland contributed approximately 39%, 22%, and 19% of the dataset, respectively, whereas all other biomes combined accounted for 20% of the dataset. A majority of the field sites are located in North America, Europe, and Asia, and a relatively small number of observations are in South America, Africa, North Asia, Australia, and Antarctica. For data points without coordinate information being reported, we searched the geographical coordinates based on the location of the study site, city, state, and country. Then, the geographical information was used for locating the sampling points on the global map to extract climate, edaphic properties, plant productivity, and soil microclimate long-term data from global datasets.

2.2. Climate, plant, and soil data

MAT and MAP with the spatial resolution of 30 s during 1970–2000 were obtained from the WorldClim database version 2 (https://www.worldclim.org/data/worldclim21.html). In addition, monthly mean SM and soil temperature (ST) during 1979–2014 were obtained from the NCEP/DOE AMIP-II Reanalysis (https://www.esrl.noaa.gov/psd/data/gridded/data.ncep.reanalysis2.gaussian.html). The global vegetation distribution data were obtained from a spatial map of 11 major biomes: boreal forest, temperate forest, tropical/subtropical forest, mixed forest, grassland, shrub, tundra, desert, natural wetlands, cropland, and pasture, which have been used in our previous publications (Xu et al., 2013, 2017). We also obtained the data of soil pH, sand, silt, clay, and SOC from the Harmonized World Soil Database (HWSD, https://daac.ornl.gov/cgi-bin/dsviewer.pl?ds_id=1247) at a 0.5 ° × 0.5 ° resolution grid. Soil bulk density and TN were extracted from the IGBP-DIS dataset (IGBP, https://daac.ornl.gov/SOILS/guides/igbp-surf
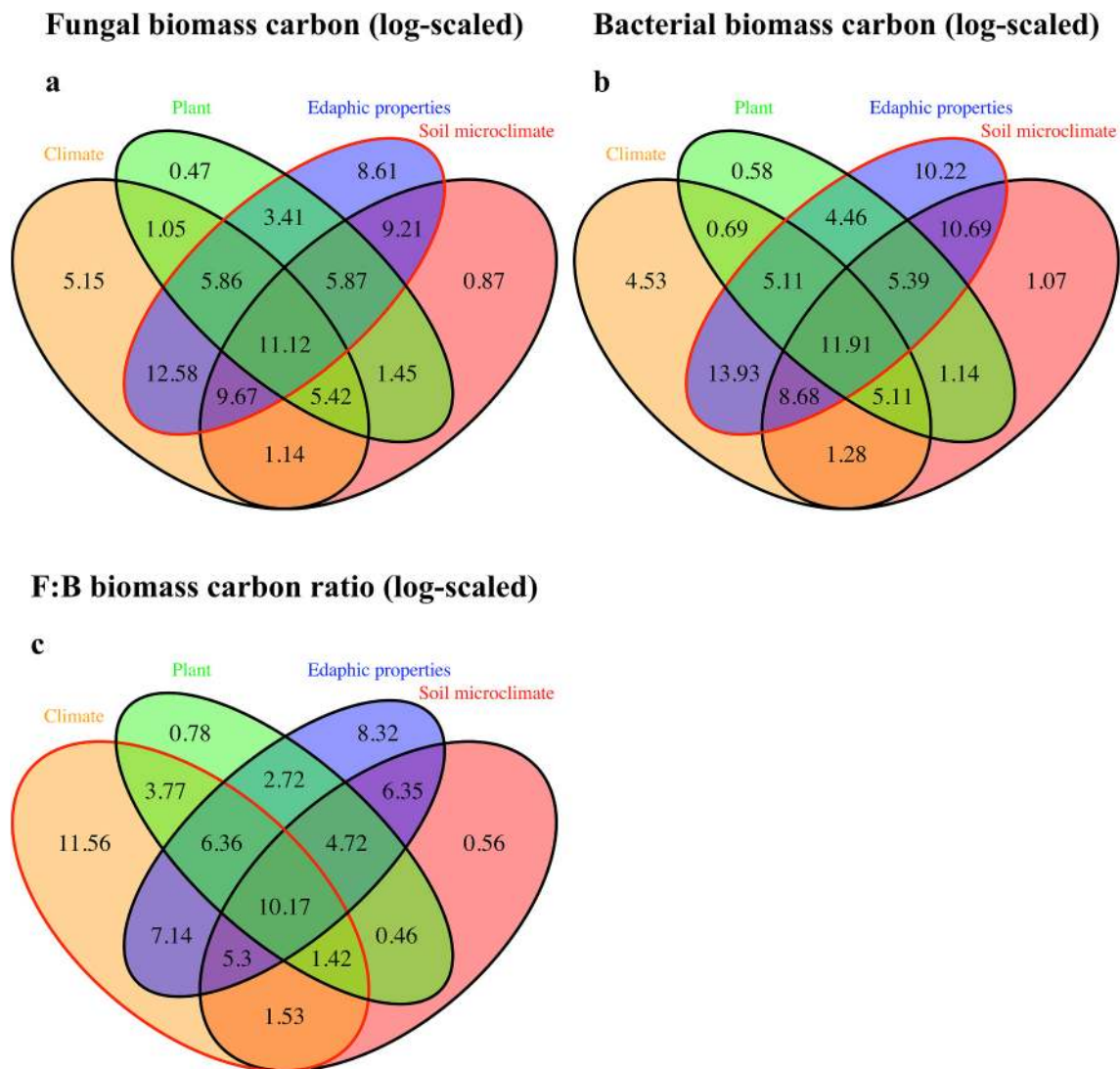
aces.html), at a spatial resolution of 0.5′ × 0.5′. Since TN in IGBP-DIS are for the 0–100 cm soil profile as a whole, we used the factor calculated from the fraction of SOC in the top 0–30 cm in the HWSD database. Since SOC and soil TN exhibit large spatial heterogeneities, and the variation in fine-scale variation in edaphic properties are underrepresented in global datasets, we examined the relationships of FBC, BBC, and F:B ratio with SOC, TN, and C:N ratio with the data directly extracted from literature. Due to the poor correlation between bulk density extracted from HWSD and the reported bulk density values in the literature, we used the same soil bulk density values for the entire top 100 cm soil profile from IGBP, assuming no difference in bulk density between top 0–30 cm and 30–100 cm soil profiles. Root C density (C_{root}) data were extracted from global dataset of 0.5° resolution based on observational data (Ruesch and Gibbs, 2008; Song et al., 2017). Annual net primary productivity (NPP) for the period of 2000–2015 was obtained from the MODIS gridded dataset with a spatial resolution of 30 s (http://files.ntsg.umt.edu/data/NTSG_Products/). These global datasets of varied spatial resolutions were interpolated to 0.5° using "bilinear" method based on the GDAL library (GDAL Development Team, 2018) for generating the global maps of FBC, BBC, and F:B ratio.

2.3. Model selection and validation

For FBC, BBC, and the F:B ratio, we developed generalized linear models considering the interactive roles of climate (MAP and MAT), soil microclimate (ST and SM), plant (NPP and C_{root}), and edaphic properties (clay, sand, soil pH, bulk density, SOC, and TN) to tease apart the controlling factors on fungal and bacterial distribution. Based on the generalized linear model of climate, plant, edaphic properties, and soil microclimate for FBC, BBC, and the F:B ratio, over 70% of the variation in FBC, BBC, and the F:B ratio was explained by the generalized linear model, and FBC and BBC were better explained than the F:B ratio (Fig. 2).

Considering the higher proportion of missing data in FBC (14.8%) and BBC (16.3%) relative to the F:B ratio (1.9%), we built an empirical model for the F:B ratio by randomly splitting the dataset with 75% of the data used in training the model. With the generalized linear model of the F:B ratio, we performed the principal component analysis to estimate the number of the important components in explaining the variations in the F:B ratio. Based on the variations explained by each component and the cumulative variation of components, we selected 31 of the most important factors, with 33.0% of the variation in the F:B ratio explained by the empirical model (Fig. S7; Table S2). The selected empirical model had the formula: $\log_{10}$ (F:B ratio) = 0.6789–0.03402 × MAT - 0.000058 × MAP + 0.003772 × ST + 1.542 × SM - 0.00099 × NPP + 0.01553 × C_{root} + 0.1226 × bulk density + 0.05991 × soil pH - 0.03631 × clay - 0.0045 × sand +0.002878 × SOC - 0.01607 × TN + 0.000177 × MAT × ST - 0.03955 × MAT × SM - 0.000015 × MAP × ST - 0.000335 × MAP × SM + 0.000005 × MAT × NPP - 0.001615 × MAT × C_{root} + 0.000001 × MAP × NPP + 0.000007 × MAP × C_{root} + 0.02201 × MAT × bulk density - 0.003794 × MAT × soil pH + 0.002188 × MAT × clay + 0.000137 × MAT × sand - 0.000061 × MAT × SOC + 0.00513 × MAT × TN - 0.000029 × MAP × soil pH + 0.000001 × MAP × clay + 0.000003 × MAP × sand - 0.000001 × MAP × SOC - 0.000043 × MAP × TN.

After the model was developed, we used 25% of the data that were not used in model development to validate the model, and we found a high consistency between model prediction and observed data (Fig. S8a). We then investigated the F:B ratio model performance by comparing the model simulated values and observed data in each biome (Fig. S9). We found good consistency between the simulated and observed log-transformed F:B ratio in all biomes except desert. Given the much lower BBC and FBC in deserts, this inconsistency does not introduce a large bias to the large-scale estimation of BBC and FBC. Additionally, we found some overestimation of the F:B ratio in croplands and pastures, indicating large uncertainties in managed systems.

Fungal biomass carbon (log-scaled)

Bacterial biomass carbon (log-scaled)

F:B biomass carbon ratio (log-scaled)

Fig. 2. Interactive effects of climate, plant, edaphic properties, and soil microclimate on (a) fungal biomass carbon (n = 611), (b) bacterial biomass carbon (n = 619), and (c) F:B ratio (n = 748); Ellipses represent the different groups of factors (climate, plant, edaphic properties, and soil microclimate). Climate includes MAT and MAP; Plant represent combined information of C_{root} and NPP; Edaphic properties includes bulk density, soil pH, SOC, ST, clay, and sand. Soil microclimate represents ST and SM (red ellipse indicates the dominant group of variables). Numbers represents the variation partitioned by different sections. (For interpretation of the references to color in this figure legend, the reader is referred to the Web version of this article.)

2.4. Mapping global soil bacterial and fungal biomass carbon

We compared the soil microbial biomass C reported in Xu et al. (2013) and the sum of FBC and BBC in this study and found a strong agreement in these estimates (Fig. S8b; R^2 = 0.91). This indicated that the sum of FBC and BBC constituted a constant proportion of microbial biomass, which provided a feasible way to estimate FBC and BBC. Based on the microbial biomass C dataset in Xu et al. (2013) and the global map of the F:B ratio generated in this study, we produced the global maps and estimated global storage of FBC and BBC. The auxiliary data used included global vegetation distribution (Xu et al., 2013) and global land area database supplied by surface data map generated by the Community Land Model 4.0 (https://svn-ccsm-models.cgd.ucar.ed u/clm2/trunk_tags/clm4_5_1_r085/models/lnd/clm/tools/clm4_5/m ksurfdata_map/).

2.5. Uncertainty analysis

To estimate the parameter-induced uncertainties in fungal and bacterial biomass distribution and storage, we used an improved Latin

Hypercube Sampling (LHS) approach to estimate variation in F:B ratio. The LHS approach is able to randomly produce an ensemble of parameter combinations with a high efficiency. This approach has been widely used to estimate uncertainties in model output (Haefner, 2005; Xu, 2010; Xu et al., 2014). Specifically, we assumed that all parameters followed a normal distribution. Then, we used LHS to randomly select an ensemble of 3000 parameter sets using the function of "improvedLHS" in the R package "lhs" (Carnell and Carnell, 2019) (Table S2). Finally, we calculated the 95% confidence interval of fungal and bacterial biomass C density and storage for reporting (Table 2).

2.6. Statistical analysis

We first tested the normality of data distribution using the function of "shapiro.test" in the R package "stats" (R Core Team, 2013). We found that FBC, BBC, and F:B ratio in our dataset did not follow a normal distribution. Therefore, these variables were log-transformed for subsequent statistical analysis. The mean and 95% confidence boundaries of FBC, BBC, and F:B ratio were transformed back to the original values for reporting. We constructed a generalized linear model using the function

Table 2
Biome- and global level storage and density of soil fungal and bacterial biomass C (95% confidence interval are shown in the bracket).

Biome	Area (million km²)	Biomass C Density (g C m⁻²)		Biomass C Storage (Pg C)	
		Fungi	Bacteria	Fungi	Bacteria
Boreal forest	11.82	304.44 (191.19–356.01)	58.66 (7.02–171.86)	3.60 (2.26–4.21)	0.69 (0.08–2.03)
Temperate forest	12.89	88.89 (40.25–115.74)	29.88 (3.01–78.5)	1.15 (0.52–1.49)	0.39 (0.04–1.01)
Tropical/Subtropical forest	16.44	64.42 (2.09–115.49)	51.58 (0.51–113.82)	1.06 (0.03–1.90)	0.85 (0.01–1.87)
Grassland	12.16	88.69 (20.55–132.48)	46.14 (2.34–114.23)	1.08 (0.25–1.61)	0.56 (0.03–1.39)
Shrub	8.11	48.06 (11.40–64.78)	17.31 (0.59–53.85)	0.39 (0.09–0.53)	0.14 (0.00–0.44)
Tundra	5.75	226.96 (150.89–256.46)	32.65 (3.13–108.08)	1.31 (0.87–1.48)	0.19 (0.02–0.62)
Desert	13.51	59.04 (14.05–74.00)	15.28 (0.32–60.21)	0.80 (0.17–1.00)	0.21 (0.00–0.81)
Natural wetlands	6.91	70.44 (30.9–99.91)	32.96 (3.47–72.44)	0.49 (0.21–0.69)	0.23 (0.02–0.50)
Cropland	14.94	67.61 (18.18–95.92)	30.09 (1.73–79.35)	1.01 (0.27–1.43)	0.45 (0.03–1.19)
Pasture	27.00	62.34 (24.03–84.12)	23.68 (1.85–61.62)	1.68 (0.65–2.27)	0.64 (0.05–1.66)
Globe	129.55	96.92 (51.23–126.75)	33.50 (3.66–79.19)	12.56 (6.64–16.42)	4.34 (0.47–10.26)

of "glm" in the R package "stats" (R Core Team, 2013) to investigate relationships between FBC, BBC, and the F:B ratio and long-term climate (MAP and MAT), soil microclimate (ST and SM), plant (NPP and C_{root}), and edaphic properties (clay, sand, soil pH, bulk density, SOC, and TN). We used Akaike information criterion (AIC) as a model selection criterion. Before conducting the generalized linear model, we tested the multicollinearity for the variables within and among each variable group, i.e., climate, soil microclimate, edaphic properties, and plant, and we found no significant multicollinearity (VIF < 5). All statistical analyses were performed and relevant figures were plotted using "agricolae" (de Mendiburu and de Mendiburu, 2019), "multcomp" (Hothorn et al., 2016), "soiltexture" (Moeys, 2018), "VennDiagram" (Chen and Boutros, 2011), "ggplot2" (Wickham et al., 2016), and "basicTrendline" (Mei et al., 2018) packages in R version 3.5.3 for Mac OS X (https://www.r-project.org). Figs. 1 and 3 were produced with NCAR Command Language (version 6.3.0) and ArcGIS (version 10.5), respectively.

3. Results

3.1. Biome-level FBC, BBC, and F:B ratio

There was a large variation in biome-level FBC, BBC, and F:B ratio (Table 1; $P < 0.001$ for FBC, BBC, and F:B ratio among biomes). Desert exhibited the lowest FBC of 16.9 (95% range: 14.4–19.9) mg kg⁻¹ and BBC of 6.8 (6.1–7.7) mg kg⁻¹, while tundra habitats displayed the highest FBC of 3683.6 (1678.5–8083.9) mg kg⁻¹ and BBC of 428.4 (237.0–774.3) mg kg⁻¹. Boreal forest had significantly higher FBC than tropical/subtropical forests and temperate forests (1234.0 mg kg⁻¹ for boreal forests vs. 258.4 mg kg⁻¹ for temperate forests and 451.4 mg kg⁻¹ for tropical/subtropical forests). Boreal forest and tropical/subtropical forests had significantly higher BBC than temperate forests (226.4 mg kg⁻¹ for boreal forest, 210.9 mg kg⁻¹ for tropical/subtropical forest vs. 53.0 mg kg⁻¹ for temperate forest), but no significant differences in BBC were found between boreal forests and tropical/subtropical forests (Table 1). Pasture had significantly higher FBC and BBC than grasslands (632.2 mg kg⁻¹ soil vs. 215.2 mg kg⁻¹ soil for FBC and 270.7 mg kg⁻¹ soil vs. 62.7 mg kg⁻¹ soil for BBC). While we did not find differences in FBC across unvegetated ground, cropland, shrub, savanna, and natural wetlands, BBC was significantly higher in wetlands than in unvegetated ground (Table 1).

The F:B ratio varied less across biomes, with the lowest values in savannas and highest values in tundra habitats (1.8 for savanna vs. 8.6 for tundra). We also found significantly higher F:B ratios in boreal forests and temperate forests than in tropical/subtropical forests (5.0 for boreal forest, 4.9 for temperate forest vs. 2.2 for tropical/subtropical forest). No significant differences in F:B ratio were found among natural wetlands, unvegetated grounds, desert, and shrub (Table 1).

3.2. Quantitative assessment of controls on microbial biogeography

We constructed generalized linear models to disentangle the effects of climate (MAP and MAT), plant (NPP and C_{root}), soil microclimate (SM and ST), and edaphic properties (SOC, TN, soil pH, clay, sand, and bulk density) on the variation in FBC, BBC, and F:B ratio. The variance inflation factor (VIF) test showed no multicollinearity among variables. Environmental factors in total explained a large proportion of variation in microbial biomass (81.9% for FBC, 84.8% for BBC, and 71.2% for F:B ratio) (Fig. 2). Notably, the edaphic properties are the most important drivers in FBC and BBC, with 66.4% and 70.4% of the variation in FBC and BBC explained by edaphic properties and the interaction with other factors, respectively (Fig. 2a and b). Complex interactions between the groups of variables explained 23.7% of the variation in FBC (Fig. 2a). In contrast, variation in BBC was explained primarily by the interactions between edaphic properties and climate (13.9%), multiple interaction terms (11.9%), and edaphic properties alone (10.2%). Climate alone and climate interactions with other variables explained 11.6% and 35.5% of the variation in the F:B ratio, respectively (Fig. 2c).

3.3. Global carbon storage of fungal and bacterial biomass

Based on our findings of environmental controls on FBC and BBC at the biome and global scales, we further developed an empirical model for the F:B ratio considering the higher proportion of missing data in FBC (14.8%) and BBC (16.3%) relative to the F:B ratio (1.9%) (Materials and Methods; Table S2). Combined with a global microbial biomass C dataset reported by Xu et al. (2013), we further produced global maps of BBC and FBC in topsoil (Fig. 3). The global FBC and BBC are estimated to be 12.56 (6.64~16.42) Pg C and 4.34 (0.47~10.26) Pg C, respectively, in 0–30 cm topsoil. Taking the global estimates of SOC (684–724 Pg C in 0–30 cm), approximately 1.8% and 0.6% of SOC is stored in soil fungi and bacteria, respectively. The highest FBC density occurs in northern high-latitude regions while the lowest values are characteristic of mid-latitude regions (Fig. 3b). Similarly, the highest BBC is found in high-latitude and equatorial regions, and the lowest in mid-latitude regions (Fig. 3c).

At biome-level, boreal forest stores the largest FBC (3.60 Pg C) and tropical/subtropical forests have the largest BBC storage (0.85 Pg C), while shrubs contribute the least to both FBC and BBC (0.39 Pg C for FBC and 0.14 Pg C for BBC) (Table 2). Although boreal forests do not occupy the Earth's largest surface area (11.82 million km²), the high FBC density contributes to its prominent FBC storage. The high microbial C in the pasture biome reflect its large area (27.0 million km²). Along with the second largest area (16.44 million km²), tropical/subtropical forests thus stored the largest BBC across the globe. The smallest FBC and BBC storage in shrub was primarily due to its small area (8.11 million km²) and the low FBC and BBC densities (48.06 g C m⁻² for FBC and 17.31 g C m⁻² for BBC). The small FBC and BBC storage in deserts primarily resulted from their low FBC and BBC densities (Fig. S5), while the small
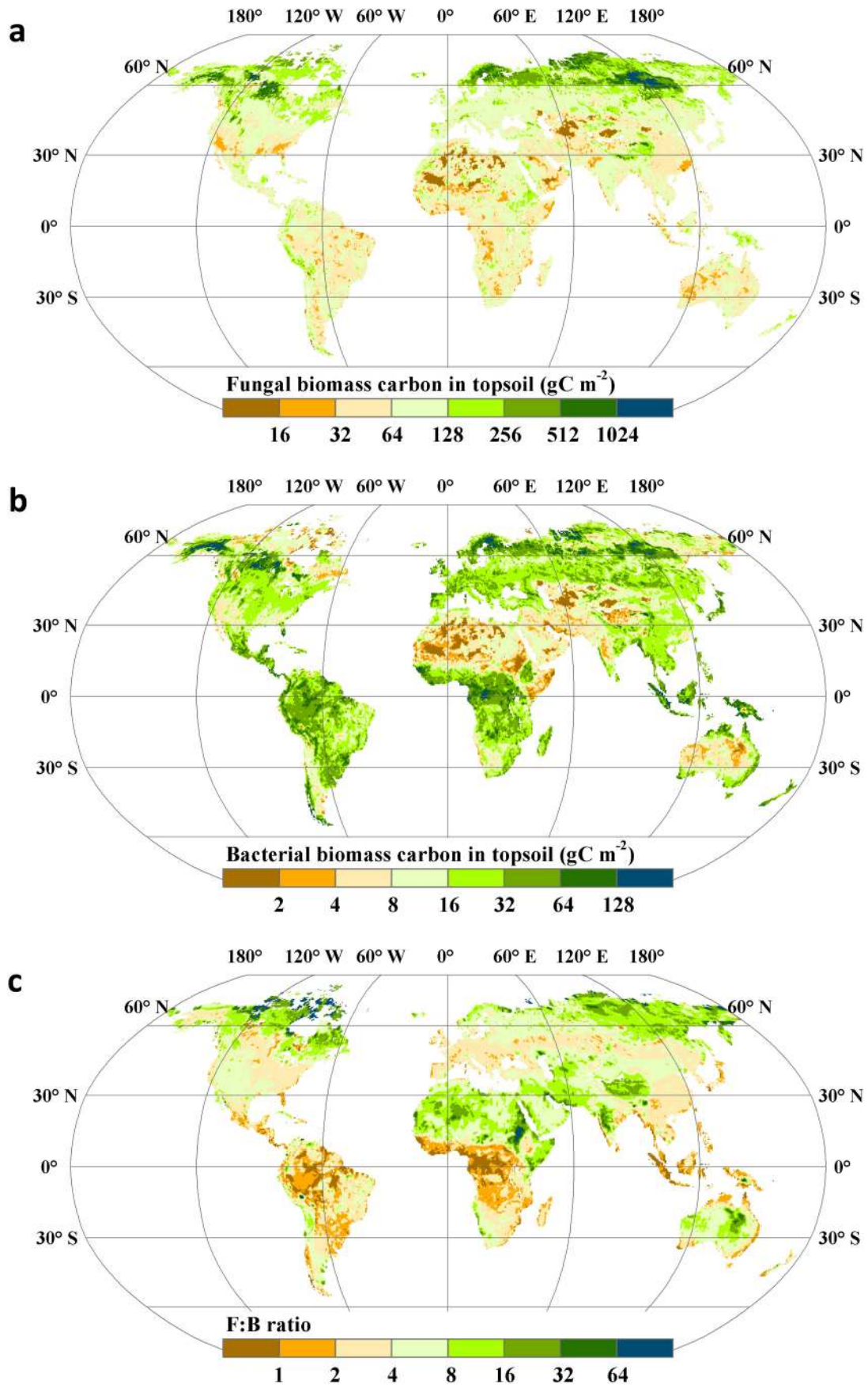
Fig. 3. Global maps of (a) fungal biomass C, (b) bacterial biomass C, and (c) F:B ratio in topsoil.

FBC and BBC storage in tundra and natural wetland may be due to the small area (5.75 million km^2 for tundra and 6.91 million km^2 for natural wetlands). Tundra has high densities of FBC and BBC (226.96 g C m^{-2} for FBC and 32.65 g C m^{-2} for BBC).

4. Discussion

4.1. Biogeographic patterns of microbial biomass

We found significant global patterns of fungi, bacteria and their balance in topsoil along latitude, climate (MAP and MAT), plant (NPP and C$_{root}$), soil microclimate (SM and ST), and edaphic factors (SOC, TN, C:N ratio, soil pH, soil texture, and bulk density) (Figs. S2–6) that are consistent with previous studies (Fierer et al., 2009; Waring et al., 2013; Chen et al., 2016; Bahram et al., 2018). For example, Bahram et al. (2018) reported the inverse unimodal trend of BBC and positive linear trend of F:B ratio along latitude and significant positive linear trend of F:B ratio along MAP and MAT. Fierer et al. (2009) reported significant controls of plant NPP on microbial biomass, whereas Waring et al. (2013) showed that F:B ratio increased along with the increase in C:N ratio, and de Vries et al. (2012) found that finely textured soils tend to have higher fungal and bacterial biomass. The key advantage of our study is that all these analyses are incorporated into a single study with much improved global sampling.

The discrepancies between this study and previous studies primarily lie in two aspects. First, in contrast to the inverse unimodal trend of FBC along latitude, Bahram et al. (2018) found a positive linear relationship between FBC and latitude, which we attribute to a small number of data points in the high-latitudes and the lack of data from high arctic habitats. Furthermore, the difference in overall sample size may have led to the variations in the relationships obtained among studies. The dataset in Bahram et al. (2018) was compiled using globally selected sampling plots (145 topsoil samples), while the dataset in this study is a comprehensive dataset with 1323 data points (Fig. 1). Second, we observed the inverse unimodal relationship between F:B ratio and soil pH, with lowest the F:B ratio at pH ~6.3, while Chen et al. (2015) reported a significant positive relationship between F:B ratio and soil pH for the Mongolian Plateau and Eskelinen et al. (2009) found a negative relationship between F:B ratio and soil pH in the alpine tundra of northern Europe. These discrepancies may result from differences in the spatial scale and range of soil pH. Soil pH values exceeded 6.5 and ranged from 4.7 to 7.0 in the studies of Chen et al. (2015) and Eskelinen et al. (2009), respectively. In their range of measurements, these F:B ratio and soil pH relationships are consistent with our study.

We found lowest FBC and BBC in deserts among biomes (Table 1), which was in line with precious studies. For example, Fierer et al. (2009) and Xu et al. (2013) also reported lowest soil microbial biomass in deserts, the low SOC concentration may result in low FBC and BBC in deserts (Fig. S6). Furthermore, both FBC and BBC were significantly higher in tropical/subtropical forests than in temperate forests among forest biomes in this study (Table 1). In contrast, we found the highest soil microbial biomass in tundra, and soil microbial biomass was significantly higher in boreal forests than that in temperate forests and tropical/subtropical forests in our previous study (Xu et al., 2013). Fierer et al. (2009) reported the higher soil microbial biomass in temperate and tropical forests than that in boreal forests, which exhibited opposite patterns with this study. The seasonality of FBC and BBC could be the cause of this inconsistency. Microbial biomass showed strong seasonal dynamics, samples taken in growing and non-growing seasons are expected to have distinct microbial biomass C density (Lipson et al., 2002).

We have also detected that F:B ratio was distinct among biomes, with the smallest F:B ratio in savanna and the highest in tundra (Table 1). Similar to our findings, Bahram et al. (2018) found significantly higher F:B ratio in boreal-arctic biomes (e.g., tundra and boreal forests) and temperate biomes (e.g., temperate forests and grassland) than tropical

biomes (e.g., savanna and tropical/subtropical forests). The highest F:B ratio in tundra may result from several reasons. First, saprotrophic fungi have more efficient enzymatic machinery than bacteria to decompose complex organic material with high C:N ratio (de Vries et al., 2012; Chen et al., 2015). Second, highly carbon-rich soils usually display low soil pH that is relatively more stressful for bacteria compared with fungi (Eskelinen et al., 2009; Rousk et al., 2010). Third, fungi are better adapted to low-temperature conditions than bacteria (Pietikäinen et al., 2005). These three interacting mechanisms may favor fungi-dominated ecosystem C and nutrient cycling in tundra and boreal forest biomes. In contrast, Fierer et al. (2009) reported a higher F:B ratio in temperate forests than tundra, but different methods used to quantify the F:B ratio may explain these differences. The F:B ratio reported in Fierer et al. (2009) was calculated as fungal to bacterial small-subunit rRNA gene copies measured using qPCR.

4.2. Spatial distribution and budget of FBC and BBC

Densities of both FBC and BBC were highest in arctic regions and lowest in mid-latitude regions globally (Fig. 3a and b). Importantly, much of the variation in FBC and BBC was determined by edaphic properties (Fig. 2a and b), indicating that the variation in edaphic factors along a latitudinal gradient may explain the global distribution of FBC and BBC. The predominant role of edaphic factors in regulating FBC and BBC can be ascribed to the impacts of soil pH, SOC, nutrient concentration, and soil water content on fungal and bacterial physiology (Brockett et al., 2012; de Vries et al., 2012). Our models revealed that We found well-predicted FBC and BBC along SOC, TN, C:N ratio, bulk density, soil pH, and soil texture (Fig. S6). In addition, the interactions between fungi and bacteria may affect spatial distribution of FBC and BBC. Although the taxonomic diversity of fungi and bacteria are highest in mid-latitude regions (Tedersoo et al., 2014; Bahram et al., 2018), these biomes support the lowest microbial biomass. Severe competition or substrate limitation in mid-latitude regions may reduce soil microbial biomass.

Generally, we found that the F:B ratio was low in low-latitudes (Fig. S2c). The decrease of soil nutrient cycling in ectomycorrhizal habitats (Fernandez and Kennedy, 2016) may result in the gradual increase of F:B ratio along latitude (Soudzilovskaia et al., 2019; Crowther et al., 2019). However, we did observe some high F:B ratios grids around equatorial regions, the high F:B ratio in these regions might be explained by several reasons. First, sand content in equator regions is much higher than other regions due to the long period of soil development and clay leaching, sandy texture soil cannot provide good protection for bacterial predators despite the relatively low bacterivore and fungivore nematode concentration in low-latitude regions (Hassink, 1992; Hoogen et al., 2019), which will increase the proportion of bacteria being consumed. Second, well-weathered soils contain low phosphorus concentration, which is known to be an important control of initial litter decay in the tropics. Fungi are capable of decomposing recalcitrant organic matter (van der Heijden et al., 2008), and thus the poor-quality litter may in return facilitate the dominance of fungi.

We estimated FBC and BBC storage in topsoil as 12.56 Pg C and 4.34 Pg C, respectively (Table 2). This result is consistent with overall terrestrial biomass estimates of FBC and BBC storage of 12 Pg C and 7 Pg C, respectively, as reported by Bar-On et al. (2018). Differences in methods probably account for most of the differences between the results reported in these studies. Fungi are more sensitive to anoxic conditions, and bacteria and archaea are important components in deep soils such as subsurface environments (Bar-On et al., 2018). It is likely that the differences in the soil depths between this study (0–30 cm) and Bar-On et al. (2018) (entire soil profile) might underpin the discrepancy in estimated global budgets of BBC.

4.3. Implications for global carbon cycle

We estimated the ratio of FBC and BBC to SOC as 1.8% and 0.6%, respectively, which agrees with the findings that microbial biomass C generally comprises 0.5–13% of SOC (Insam, 1990; Sparling, 1992; Geisseler and Scow, 2014; Ananyeva et al., 2015). Soil microbes have a much faster turnover rate than soil organic carbon (Xu et al., 2017). Fungi and bacteria account for >90% of the total soil microbial biomass and are the major decomposer groups in soils (Beare, 1997). Necromass of fungi and bacteria is one of the major sources of recalcitrant organic compounds in soil (Gougoulias et al., 2014). Soil microbial necromass is about three orders of magnitude higher than soil microbial biomass (Glaser et al., 2004), and can make up more than half of SOC (Liang et al., 2019). Fungal-derived necromass was reported to be dominant over the bacterial-derived necromass in SOC formation, which may be due to the higher recalcitrance of their cell walls, the biosynthesis of secondary metabolites, and the hyphae structure facilitated mineral protection (Li et al., 2015).

In addition to the formation of recalcitrant organic compounds in soil, soil fungal and bacterial biomass are important in conducting biochemical transformation of C and nutrients (Xu et al., 2013). For example, as litter quality decreases, fungi are expected to play more important roles (Van Der Heijden et al., 2018). Therefore, variations in F:B ratios can imply changes in the decomposer population and the changes in soil microbial community composition and function (Six et al., 2006).

However, the balance between fungal and bacterial biomass (F:B ratio) was in large variation. In addition to the natural variations due to the seasonal dynamics of fungal and bacterial biomass, fungal and bacterial growth are affected by temperature, moisture, soil pH, substrate, vegetation, and toxicity (Rousk and Bååth, 2011). Therefore, F:B ratios are highly vulnerable to changing environmental conditions such as climate change, land use change, pollution and soil contamination. For example, Bell et al. (2014) found that a 7-year period of surplus watering increased soil F:B ratio due to the deficiency of phosphorus in watered plots. Either fungal or bacterial dominance is closely associated with the cycling pace of organic carbon from soil to atmosphere (Carvalhais et al., 2014; Crowther et al., 2019). Therefore, the F:B ratio is one critical indicator of global C cycle under the changing environment.

4.4. Limitations and prospects

Some limitations need to be recognized when interpreting the results. First, we assumed that all samples were taken from surface soil, representing 0–30 cm soil profile; while the sampling depth varies between 0 and 30 cm in this study, with 76% of soil samples taken for topsoil of 0–15 cm. Considering the vertical distribution of microbial biomass C (Xu et al., 2013), this bias might lead to a slight overestimation in BBC and FBC. Second, the disproportionate number of data points from each biome relative to its land area might lead to bias in spatial extrapolation. For example, the data points from forest, grassland, and cropland contribute approximately 80% of the dataset, while the land area of these biomes is approximately 50% of the global land area (Table 2). Third, the sampling date might be another reason for uncertainty; the data points were taken from various seasons and we assume the average across seasons represent the annual mean. In this aspect, future studies on seasonal variation of soil FBC and BBC should address this limitation. Fourth, actinobacteria were categorized as bacteria in a portion of studies but not in others (Andersen et al., 2010; Royer-Tardif et al., 2010). Although we reclassified bacteria based on the biomarkers used in the literature, i.e., actinobacteria were added into bacteria if the papers did not use general bacterial markers (e.g., PLFAs 14:0, 15:0, 16:0, 17:0, and 18:0) for the reported bacterial PLFA concentration, the diverse classification may introduce minor uncertainties in simulating the relationships between FBC and BBC.

5. Conclusions

This study reported the BBC and FBC in major biomes and produced the first global maps of BBC and FBC in 0–30 cm topsoil. The global FBC and BBC are estimated to be 12.56 (6.64–16.42) Pg C and 4.34 (0.47–10.26) Pg C, respectively, in 0–30 cm topsoil. The FBC, BBC, and F:B ratio showed clear spatial patterns on a global scale. Significant trends are observed along meteorological parameters (MAP, MAT, ST, and SM), vegetation productivity (C_{root} and NPP), and edaphic properties (soil texture, bulk density, soil pH, SOC, TN, and C:N ratio). The FBC and BBC were primarily determined by edaphic properties including soil texture, soil pH, bulk density, and SOC. the F:B ratio is primarily driven by climatic variables, particularly MAP and MAT. The biogeographic patterns of BBC and FBC suggest that multiple mechanisms synergistically affect soil C and nutrient cycling at the global scale. The biogeographic patterns of BBC and FBC and their controls facilitate the development of microbial macroecology (Xu et al., 2020) and provide fundamental information for incorporating microbial mechanisms into Earth system models, and the estimated budget and maps of BBC and BGC at biome and global scales serve as a benchmark for validating microbial models.

Data Availability

The final maps of the soil fungal and bacterial biomass are archived at Dryad repository https://doi.org/10.5061/dryad.qrfj6q5db. The data sources for the meteorology, soil properties and microbial properties can be found in the Materials and Methods section.

Code availability

The code for data analysis and producing global maps for the bacteria and fungi can be accessed upon request to L.H. and X.X.

Declaration of competing interest

The authors declare that they have no known competing financial interests or personal relationships that could have appeared to influence the work reported in this paper.

Appendix A. Supplementary data

Supplementary data to this article can be found online at https://doi.org/10.1016/j.soilbio.2020.108024.

References

Ananyeva, N.D., Castaldi, S., Stolnikova, E.V., Kudeyarov, V.N., Valentini, R., 2015. Fungi-to-bacteria ratio in soils of European Russia. Archives of Agronomy and Soil Science 61, 427–446.

Andersen, R., Grasset, L., Thormann, M.N., Rochefort, L., Francez, A.-J., 2010. Changes in microbial community structure and function following Sphagnum peatland restoration. Soil Biology and Biochemistry 42, 291–301.

Aon, M.A., Cabello, M.N., Sarena, D.E., Colaneri, A.C., Franco, M.G., Burgos, J.L., Cortassa, S., 2001. I. Spatio-temporal patterns of soil microbial and enzymatic activities in an agricultural soil. Applied Soil Ecology 18, 239–254.

Bahram, M., Hildebrand, F., Forslund, S.K., Anderson, J.L., Soudzilovskaia, N.A., Bodegom, P.M., Bengtsson-Palme, J., Anslan, S., Coelho, L.P., Harend, H., 2018. Structure and function of the global topsoil microbiome. Nature 560, 233.

Bar-On, Y.M., Phillips, R., Milo, R., 2018. The biomass distribution on Earth. Proceedings of the National Academy of Sciences 115, 6506–6511.

Beare, M.H., 1997. Fungal and bacterial pathways of organic matter decomposition and nitrogen mineralization in arable soils. Soil Ecology in Sustainable Agricultural Systems 37–70.

Beare, M.H., Neely, C.L., Coleman, D.C., Hargrove, W.L., 1990. A substrate-induced respiration (SIR) method for measurement of fungal and bacterial biomass on plant residues. Soil Biology and Biochemistry 22, 585–594.

Bell, C.W., Tissue, D.T., Loik, M.E., Wallenstein, M.D., Martinez, V.A., Erickson, R.A., Zak, J.C., 2014. Soil microbial and nutrient responses to 7 years of seasonally altered precipitation in a Chihuahuan Desert grassland. Global Change Biology 20, 1657–1673.

Birkhofer, K., Bezemer, T.M., Bloem, J., Bonkowski, M., Christensen, S., Dubois, D., Ekelund, F., Fließbach, A., Gunst, L., Hedlund, K., 2008. Long-term organic farming fosters below and aboveground biota: Implications for soil quality, biological control and productivity. Soil Biology and Biochemistry 40, 2297–2308.

Boer, W.D., Folman, L.B., Summerbell, R.C., Boddy, L., 2005. Living in a fungal world: impact of fungi on soil bacterial niche development. FEMS Microbiology Reviews 29, 795–811.

Brockett, B.F.T., Prescott, C.E., Grayston, S.J., 2012. Soil moisture is the major factor influencing microbial community structure and enzyme activities across seven biogeoclimatic zones in western Canada. Soil Biology and Biochemistry 44, 9–20.

Caldwell, B.A., 2005. Enzyme activities as a component of soil biodiversity: a review. Pedobiologia 49, 637–644.

Carnell, R., Carnell, M.R., 2019. Package 'lhs'. http://cran.stat.auckland.ac.nz/web/packages/lhs/lhs.pdf.780.

Carvalhais, N., Forkel, M., Khomik, M., Bellarby, J., Jung, M., Migliavacca, M., Mu, M., Saatchi, S., Santoro, M., Thurner, M., 2014. Global covariation of carbon turnover times with climate in terrestrial ecosystems. Nature 514, 213.

Chen, D., Mi, J., Chu, P., Cheng, J., Zhang, L., Pan, Q., Xie, Y., Bai, Y., 2015. Patterns and drivers of soil microbial communities along a precipitation gradient on the Mongolian Plateau. Landscape Ecology 30, 1669–1682.

Chen, H., Boutros, P.C., 2011. VennDiagram: a package for the generation of highly-customizable Venn and Euler diagrams in R. BMC Bioinformatics 12, 35.

Chen, Y., Ding, J., Peng, Y., Li, F., Yang, G., Liu, L., Qin, S., Fang, K., Yang, Y., 2016. Patterns and drivers of soil microbial communities in Tibetan alpine and global terrestrial ecosystems. Journal of Biogeography 43, 2027–2039.

Crowther, T.W., Hoogen, J.v.d., Wan, J., Mayes, M.A., Keiser, A.D., Mo, L., Averill, C., Maynard, D.S., 2019. The global soil community and its influence on biogeochemistry. Science 365 eaav0550.

de Mendiburu, F., de Mendiburu, M.F., 2019. Package 'agricolae'. R Package Version, pp. 1–2.

de Vries, F.T., Manning, P., Tallowin, J.R.B., Mortimer, S.R., Pilgrim, E.S., Harrison, K.A., Hobbs, P.J., Quirk, H., Shipley, B., Cornelissen, J.H.C., 2012. Abiotic drivers and plant traits explain landscape-scale patterns in soil microbial communities. Ecology Letters 15, 1230–1239.

DeLong, E.F., Harwood, C.S., Chisholm, P.W., Karl, D.M., Moran, M.A., Schmidt, T.M., Tiedje, J.M., Treseder, K.K., Worden, A.Z., 2011. Incorporating microbial processes into climate models. The American Academy of Microbiology, Washington DC.

Ding, J., Zhang, Y., Wang, M., Sun, X., Cong, J., Deng, Y., Lu, H., Yuan, T., Van Nostrand, J.D., Li, D., Zhou, J., Yang, Y., 2015. Soil organic matter quantity and quality shape microbial community compositions of subtropical broadleaved forests. Molecular Ecology 5175–5185.

Eskelinen, A., Stark, S., Männistö, M., 2009. Links between plant community composition, soil organic matter quality and microbial communities in contrasting tundra habitats. Oecologia 161, 113–123.

Falkowski, P.G., Fenchel, T., Delong, E.F., 2008. The microbial engines that drive Earth's biogeochemical cycles. Science 320, 1034–1039.

Fenchel, T., 2002. Microbial Behavior in a Heterogeneous World. Science 296, 1068–1071.

Fernandez, C.W., Kennedy, P.G., 2016. Revisiting the 'Gadgil effect': do interguild fungal interactions control carbon cycling in forest soils? New Phytologist 209, 1382–1394.

Fierer, N., Jackson, R.B., 2006. The diversity and biogeography of soil bacterial communities. Proceedings of the National Academy of Sciences 103, 626–631.

Fierer, N., Strickland, M.S., Liptzin, D., Bradford, M.A., Cleveland, C.C., 2009. Global patterns in belowground communities. Ecology Letters 12, 1238–1249.

Frostegård, A., Bååth, E., 1996. The use of phospholipid fatty acid analysis to estimate bacterial and fungal biomass in soil. Biology and Fertility of Soils 22, 59–65.

GDAL Development Team, 2018. GDAL/OGR Geospatial Data Abstraction Library. Version 2.1.3.3. Open Source Geospatial Foundation. Retrieved from. http://www.gdal.org.

Geisseler, D., Scow, K.M., 2014. Long-term effects of mineral fertilizers on soil microorganisms–A review. Soil Biology and Biochemistry 75, 54–63.

Glaser, B., Turrión, M., Alef, K., 2004. Amino sugars and muramic acid—biomarkers for soil microbial community structure analysis. Soil Biology and Biochemistry 36, 399–407.

Gougoulias, C., Clark, J.M., Shaw, L.J., 2014. The role of soil microbes in the global carbon cycle: tracking the below-ground microbial processing of plant-derived carbon for manipulating carbon dynamics in agricultural systems. Journal of the Science of Food and Agriculture 94, 2362–2371.

Haefner, J.W., 2005. Modeling Biological Systems-Principles and Applications. Springer, New York.

Hanson, C.A., Fuhrman, J.A., Horner-Devine, M.C., Martiny, J.B., 2012. Beyond biogeographic patterns: processes shaping the microbial landscape. Nature Review Microbiology 10, 496–506.

Hassink, J., 1992. Effects of soil texture and structure on carbon and nitrogen mineralization in grassland soils. Biology and Fertility of Soils 14, 126–134.

Högberg, P., Nordgren, A., Buchmann, N., Taylor, A.F.S., Ekblad, A., Högberg, M.N., Nyberg, G., Ottosson-Loèfvenius, M., Read, D.J., 2001. Large-scale forest girdling shows that current photosynthesis drives soil respiration. Nature 411, 789–792.

Hoogen, J.v.d., Geisen, S., Routh, D., Ferris, H., Traunspurger, W., Wardle, D.A., Goede, R.G.M.d., Adams, B.J., Ahmad, W., Andriuzzi, W.S., Bardgett, R.D., Bonkowski, M., Campos-Herrera, R., Cares, J.E., Caruso, T., Caixeta, L.d.B., Chen, X., Costa, S.R., Creamer, R., Castro, J.M.d.C., Dam, M., Djigal, D., Escuer, M., Griffiths, B.S., Gutiérrez, C., Hohberg, K., Kalinkina, D., Kardol, P., Kergunteuil, A., Korthals, G., Krashevska, V., Kudrin, A.A., Li, Q., Liang, W., Magilton, M., Marais, M., Martín, J.A.R., Matveeva, E., Mayad, E.H., Mulder, C., Mullin, P., Neilson, R., Nguyen, T.A.D., Nielsen, U.N., Okada, H., Rius, J.E.P., Pan, K., Peneva, V., Pellissier, L., Silva, J.C.P.d., Pitteloud, C., Powers, T.O., Powers, K., Quist, C.W., Rasmann, S., Moreno, S.S., Scheu, S., Setälä, H., Sushchuk, A., Tiunov, A.V., Trap, J., Putten, W.v.d., Vestergård, M., Villenave, C., Waeyenberge, L., Wall, D.H., Wilschut, R., Wright, D.G., Yang, J.-i., Crowther, T.W., 2019. Soil nematode abundance and functional group composition at a global scale. Nature 572, 194–198.

Hothorn, T., Bretz, F., Westfall, P., Heiberger, R.M., Schuetzenmeister, A., Scheibe, S., Hothorn, M.T., 2016. Package 'multcomp'. Simultaneous Inference in General Parametric Models. Project for Statistical Computing, Vienna, Austria.

Insam, H., 1990. Are the soil microbial biomass and basal respiration governed by the climatic regime? Soil Biology and Biochemistry 22, 525–532.

Jost, D.I., Indorf, C., Joergensen, R.G., Sundrum, A., 2011. Determination of microbial biomass and fungal and bacterial distribution in cattle faeces. Soil Biology and Biochemistry 43, 1237–1244.

Klamer, M., Bååth, E., 2004. Estimation of conversion factors for fungal biomass determination in compost using ergosterol and PLFA 18: 2ω6, 9. Soil Biology and Biochemistry 36, 57–65.

Li, N., Xu, Y.-Z., Han, X.-Z., He, H.-B., Zhang, X.-D., Zhang, B., 2015. Fungi contribute more than bacteria to soil organic matter through necromass accumulation under different agricultural practices during the early pedogenesis of a Mollisol. European Journal of Soil Biology 67, 51–58.

Liang, C., Amelung, W., Lehmann, J., Kästner, M., 2019. Quantitative assessment of microbial necromass contribution to soil organic matter. Global Change Biology 25, 3578–3590.

Lipson, D.A., Schadt, C.W., Schmidt, S.K., 2002. Changes in soil microbial community structure and function in an alpine dry meadow following spring snow melt. Microbial Ecology 43, 307–314.

Martiny, J.B.H., Bohannan, B.J.M., Brown, J.H., Colwell, R.K., Fuhrman, J.A., Green, J. L., Horner-Devine, M.C., Kane, M., Krumins, J.A., Kuske, C.R., Morin, P.J., Naeem, S., Ovreas, L., Reysenbach, A.-L., Smith, V.H., Staley, J.T., 2006. Microbial biogeography: putting microorganisms on the map. Nature Review Microbiology 4, 102–112.

Mei, W., Yu, G., Lai, J., Rao, Q., Umezawa, Y., 2018. basicTrendline: Add Trendline and Confidence Interval of Basic Regression Models to Plot, 3 ed, 2.0.

Moeys, J., 2018. The Soil Texture Wizard: R Functions for Plotting, Classifying, Transforming and Exploring Soil Texture Data. CRAN. R-Project.

Mouginot, C., Kawamura, R., Matulich, K.L., Berlemont, R., Allison, S.D., Amend, A.S., Martiny, A.C., 2014. Elemental stoichiometry of Fungi and Bacteria strains from grassland leaf litter. Soil Biology and Biochemistry 76, 278–285.

Pietikäinen, J., Pettersson, M., Bååth, E., 2005. Comparison of temperature effects on soil respiration and bacterial and fungal growth rates. FEMS Microbiology Ecology 52, 49–58.

R Core Team, 2013. R: A Language and Environment for Statistical Computing. R Foundation for Statistical Computing, Vienna, Austria (Available).

Rillig, M.C., Mummey, D.L., 2006. Mycorrhizas and soil structure. New Phytologist 171, 41–53.

Rousk, J., Bååth, E., 2011. Growth of saprotrophic fungi and bacteria in soil. FEMS Microbiology Ecology 78, 17–30.

Rousk, J., Brookes, P.C., Bååth, E., 2010. Investigating the mechanisms for the opposing pH relationships of fungal and bacterial growth in soil. Soil Biology and Biochemistry 42, 926–934.

Royer-Tardif, S., Bradley, R., Parsons, W., 2010. Evidence that plant diversity and site productivity confer stability to forest floor microbial biomass. Soil Biology and Biochemistry 42, 813–821.

Ruesch, A., Gibbs, H.K., 2008. New IPCC Tier-1 Global Biomass Carbon Map for the Year 2000. Oak Ridge National Laboratory, Oak Ridge, Tennessee. Available online from: the Carbon Dioxide Information Analysis Center. http://cdiac.ornl.gov.

Schimel, J.P., Schaeffer, S.M., 2012. Microbial control over carbon cycling in soil. Frontiers in Microbiology 3, 1–11.

Six, J., Frey, S.D., Thiet, R.K., Batten, K.M., 2006. Bacterial and fungal contributions to carbon sequestration in agroecosystems. Soil Science Society of America Journal 70, 555–569.

Song, X., Hoffman, F.M., Iversen, C.M., Yin, Y., Kumar, J., Ma, C., Xu, X., 2017. Significant inconsistency of vegetation carbon density in CMIP5 Earth system models against observational data. Journal of Geophysical Research: Biogeosciences 122, 2282–2297.

Soudzilovskaia, N.A., van Bodegom, P.M., Terrer, C., Zelfde, M.v.t., McCallum, I., Luke McCormack, M., Fisher, J.B., Brundrett, M.C., de Sá, N.C., Tedersoo, L., 2019. Global mycorrhizal plant distribution linked to terrestrial carbon stocks. Nature Communications 10, 5077.

Sparling, G.P., 1992. Ratio of microbial biomass carbon to soil organic carbon as a sensitive indicator of changes in soil organic matter. Soil Research 30, 195–207.

Tedersoo, L., Bahram, M., Põlme, S., Kõljalg, U., Yorou, N.S., Wijesundera, R., Ruiz, L.V., Vasco-Palacios, A.M., Thu, P.Q., Suija, A., Smith, M.E., Sharp, C., Saluveer, E., Saitta, A., Rosas, M., Riit, T., Ratkowsky, D., Pritsch, K., Põldmaa, K., Piepenbring, M., Phosri, C., Peterson, M., Parts, K., Pärtel, K., Otsing, E., Nouhra, E., Njouonkou, A.L., Nilsson, R.H., Morgado, L.N., Mayor, J., May, T.W., Majuakim, L., Lodge, D.J., Lee, S.S., Larsson, K.-H., Kohout, P., Hosaka, K., Hiiesalu, I., Henkel, T. W., Harend, H., Guo, L.-d., Greslebin, A., Grelet, G., Geml, J., Gates, G., Dunstan, W., Dunk, C., Drenkhan, R., Dearnaley, J., Kesel, A.D., Dang, T., Chen, X., Buegger, F., Brearley, F.Q., Bonito, G., Anslan, S., Abell, S., Abarenkov, K., 2014. Global diversity and geography of soil fungi. Science 346.

Turner, B.L., Lambers, H., Condron, L.M., Cramer, M.D., Leake, J.R., Richardson, A.E., Smith, S.E., 2013. Soil microbial biomass and the fate of phosphorus during long-term ecosystem development. Plant and Soil 367, 225–234.

van der Heijden, M.G.A., Bardgett, R.D., Van Straalen, N.M., 2008. The unseen majority: soil microbes as drivers of plant diversity and productivity in terrestrial ecosystems. Ecology Letters 11, 296–310.

Van Der Heijden, M.G.A., Bardgett, R.D., Van Straalen, N.M., 2018. The unseen majority: soil microbes as drivers of plant diversity and productivity in terrestrial ecosystems. Ecology Letters 296–310.

Waring, B.G., Averill, C., Hawkes, C.V., 2013. Differences in fungal and bacterial physiology alter soil carbon and nitrogen cycling: insights from meta-analysis and theoretical models. Ecology Letters 16, 887–894.

Wickham, H., Chang, W., Wickham, M.H., 2016. Package 'ggplot2'. Create Elegant Data Visualisations Using the Grammar of Graphics, vol. 2. Version, pp. 1–189.

Xu, X., Wang, N., Lipson, D.L., Sinsabaugh, R.L., Schimel, J.P., He, L., Soudzilovskaia, N. A., Tedersoo, L., 2020. Microbial macroecology: in search of mechanisms governing microbial biogeographical patterns. Global Ecology and Biogeography. https://doi.org/10.1111/geb.13162.

Wieder, W.R., Bonan, G.B., Allison, S.D., 2013. Global soil carbon projections are improved by modelling microbial processes. Nature Climate Change 3, 909–912.

Xu, X., 2010. Modeling Methane and Nitrous Oxide Exchanges between the Atmosphere and Terrestrial Ecosystems over North America in the Context of Multifactor Global Change, School of Forestry and Wildlife Sciences. Auburn University, Auburn, p. 199.

Xu, X., Schimel, J.P., Janssens, I.A., Song, X., Song, C., Yu, G., Sinsabaugh, R.L., Tang, D., Zhang, X., Thornton, P.E., 2017. Global pattern and controls of soil microbial metabolic quotient. Ecological Monographs 87, 429–441.

Xu, X., Schimel, J.P., Thornton, P.E., Song, X., Yuan, F., Goswami, S., 2014. Substrate and environmental controls on microbial assimilation of soil organic carbon: a framework for Earth system models. Ecology Letters 17, 547–555.

Xu, X., Thornton, P.E., Post, W.M., 2013. A global analysis of soil microbial biomass carbon, nitrogen and phosphorus in terrestrial ecosystems. Global Ecology and Biogeography 22, 737–749.